International Journal of Science and Research (IJSR)
ISSN: 2319-7064
Impact Factor 2024: 7.101

Experimental Evaluation of Hydrokinetic Turbine Performance: A Comparative Study of Inlet and Outlet Channel Angles

Akhmad Nurdin[1], Zuryati Djafar[2*], Nasruddin Azis[3], Wahyu H. Piarah[4]

[1]Mechanical Engineering Department, Faculty of Industrial Technology, Universitas Balikpapan, Balikpapan – East Kalimantan 76114, Indonesia
Email: *akhmad.nurdin[at]uniba-bpn.ac.id*

[2]Mechanical Engineering Department, Faculty of Engineering, Universitas Hasanuddin, Bontomarannu, Gowa, South Sulawesi 92171 Indonesia
Email: *zuryatidjafar[at]unhas.ac.id*

[3]Mechanical Engineering Department, Faculty of Engineering, Universitas Hasanuddin, Bontomarannu, Gowa, South Sulawesi 92171 Indonesia
Email: *teknikuh[at]gmail.com*

[4]Mechanical Engineering Department, Faculty of Engineering, Universitas Hasanuddin, Bontomarannu, Gowa, South Sulawesi 92171 Indonesia
Email: *wahyupiarah[at]unhas.ac.id*

Abstract: ***The hydrokinetic turbine is a recent renewable energy technology capable of converting kinetic energy of natural water currents into mechanical and electrical power. The performance of these systems is strongly influenced by the geometry of flow-guide channel used to direct and accelerate water flow into and out of turbine. Therefore, this study investigates the performance of a horizontal-axis hydrokinetic turbine by examining the effects of nozzle inlet angles (10°, 20°, 30°) and diffuser outlet angles (10°, 13.9°, 15°) on mechanical power and energy conversion efficiency. The turbine system was tested in the Manggar River, with configurations mounted on a floating platform and towed at controlled speeds. Results showed that the 30° nozzle inlet angle yielded the highest mechanical power, while the 13.9° diffuser outlet angle achieved the best power coefficient. The findings highlight that optimal channel geometry must be chosen based on specific performance goals, such as maximizing mechanical output or improving energy conversion efficiency, offering practical guidance for deploying turbines in low-flow river environments.***

Keywords: Hydrokinetic energy; nozzle; diffuser; inlet angle; outlet angle; mechanical power; power coefficient

1. Introduction

Fossil fuels are still the primary source of electricity generation compared to renewable energy. Data from the Institute for Essential Services Reform (IESR) on February 9, 2022, showed that energy systems in Southeast Asia remained highly dependent on fossil fuels, particularly coal [1]. Although renewable energy generation capacity has increased, there is a significant rise in conventional energy consumption, such as coal [2]. The dependence persists because energy generation planning focuses mainly on market prices and coal costs, ignoring environmental impacts [3].

In this context, renewable power plants are needed to reduce environmental impacts. Previous studies have explored sources like wind, solar, hydro, geothermal, and bioenergy [4], as well as ocean wave, biomass, and nuclear energy, accompanied by cost analyses [5], [6], [7], [8], [9]. However, solar and wind are intermittent [10], while hydropower and geothermal require large initial investment [11],[12]. Hydropower is considered one of the cleanest and most efficient renewable sources [13]. Hydrokinetic plants (PLTHK) use river flow to generate electricity and have strong potential in Malaysia and Indonesia. The key challenge is limited river flow-velocity data due to low flow speeds [14].

Several investigations have been conducted to increase flow velocity in wind turbine and hydrokinetic. A previous study [15] comprehensively discussed the concept of shrouded wind turbine. In an optimization effort, this study evaluated shroud inlet angle and found that 30° obtained the best velocity augmentation compared to 45° and 60°. This result was consistent at inlet velocity of 6 m/s and 10 m/s. Another report on diffuser by [16],[17] showed a rise in flow power in wind and hydro turbine by increasing power coefficient around the rotor. This was similar to the results obtained with venturi shapes [18]. Furthermore, optimizing diffuser outlet shape using Bezier curves showed innovative hydrofoil profile configurations. Among the 1,200 solutions analyzed, the top 80 configurations had outlet angle of 13.9°, obtaining power coefficients of 98% and 118% without and with tip clearance, respectively [19]. A systematic review [20] of 155 studies on horizontal-axis turbine with diffuser additions found that 58% reported an increase in the power coefficient compared to a plain turbine of the same diameter. Design of experiments (DOE) simulation [21] showed that specific diffuser geometries could increase flow velocity by approximately 31.7% (3.62 m/s) with a curved profile on the inside. Another study [22] used CFD simulation on a Micro-Horizontal Axis Diffuser-Augmented Turbine (MHDT) system with ANSYS Fluent software and obtained an average increase in power coefficient of 0.668 at a tip speed ratio (TSR) of 4.25, compared to 0.442 for turbine without diffuser.

An optimization method based on axisymmetric Reynolds-Averaged Navier-Stokes (RANS) was also used to design ducting geometry to enhance wind turbine thrust, generating power increase of approximately 1.43 times the Betz limit [23]. Experimental study [24] on a full-scale Diffuser-Augmented Wind Turbine (DAWT) showed a velocity increase from 1.02 m/s to 2.41 m/s, and an augmentation ratio of 8.32 compared to a bare wind turbine. Furthermore, [15] numerical simulation was performed to optimize diffuser design in micro-hydrokinetic turbine. The use of response surface optimization method produced a 48% increase in power at an outlet-to-inlet area ratio. An investigation was also conducted on [25] geometry of wind turbine shrouds with variations in inlet angle and shroud profile, including ring-shaped boundary layer control methods. The results showed an increase in velocity and power by 80%, with an optimal inlet angle of approximately 30-45°.

Based on the description above, this study aims to experimentally evaluate how variations in nozzle inlet and diffuser outlet angles affect the mechanical output and efficiency of a horizontal-axis hydrokinetic turbine. The results provide critical experimental evidence for optimizing turbine design under realistic river conditions, offering design insights that are vital for advancing micro-hydro energy solutions in resource-constrained areas.

2. Methodology

This study used a full-scale experimental method designed to evaluate the influence of inlet nozzle angles and diffuser outlet angles on the performance of horizontal-axis hydrokinetic turbine. Experiments were conducted in the Manggar River, located in Manggar, East Balikpapan, Balikpapan City, East Kalimantan Province, Indonesia. The method enabled precise measurement of flow conditions, turbine dynamics, and power output. Kinetic energy from river flow was converted into electricity by rotating turbine and electromechanical converter. A horizontal-axis hydrokinetic turbine prototype was used to study how the guiding channel shape and size influence power generation. Equipment size and placement appear in Figure 1.

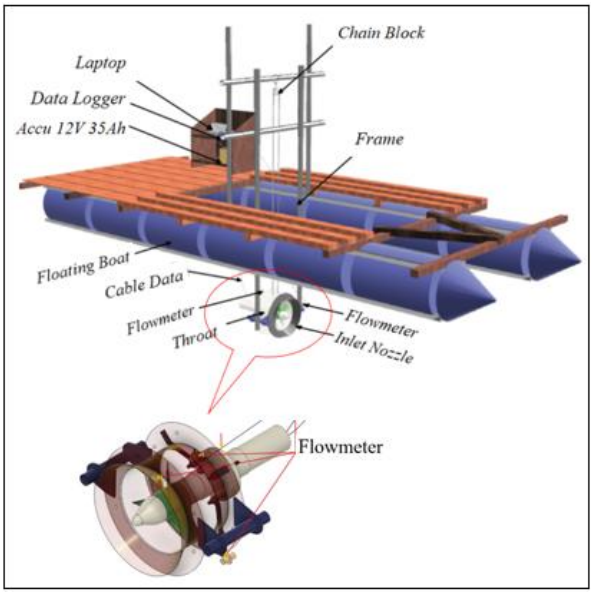

Figure 1: Hydrokinetic turbine equipment installation

All equipment and sensors were fixed to a custom floating platform to ensure correlation with the incoming flow. The platform was towed with a motorboat at controlled speed to adjust flow velocity into turbine guide channel. The turbine was operated at a depth of 1.2 meters.

Data acquisition was initiated after flow inside the guide channel reached steady-state conditions, as verified by the upstream and downstream flow meters. The primary parameters measured were flow velocity before and after the rotor, shaft rotational speed (rpm), generator output voltage and current, and pressure differentials across the channel. All data were recorded using a data logger for further analysis and interpretation. The experiments were conducted for diffuser models with outlet angles of 10°, 13.9°, and 15°, as well as nozzle models with inlet angles of 10°, 20°, and 30°.

2.1. Fundamental equation of the system

The equation for power generated by flow entering the guide channel is expressed as follows.

$$P_1 = \frac{1}{2}.\rho.A_1.{v_o}^3. \quad (1)$$

Where $P_1$is the incoming kinetic power (W), ρ is fluid density (kg/m³), A_1 is the cross-sectional area of flow (m²), and v_0 is the freestream flow velocity (m/s).

When a fluid flows through the converter at a constant mass flow rate, as shown in Figure 2.

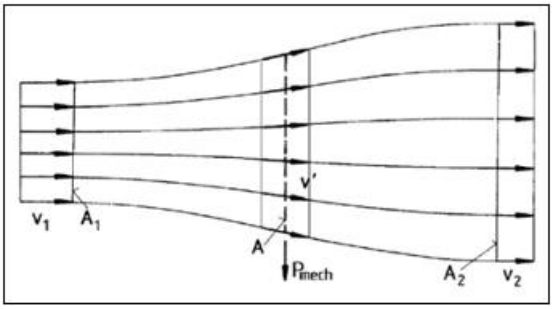

Figure 2: Mechanical energy extraction scheme in fluid flow extraction according to the basic theory of momentum [25]

As shown in Figure 2 and applying the law of conservation of momentum, the mechanical power of fluid delivered to the converter can be expressed as:

$$P_m = \frac{1}{4}.\rho.A_t.({v_1}^2 - {v_2}^2)two(v_1 + v_2). \quad (2)$$

In this equation, $A_t$is the cross-sectional area at the throat (m²), $v_1$and $v_2$are flow velocity before and after the rotor (m/s).

The power coefficient C_p, which represents the efficiency of power extraction from the available kinetic energy, is defined as.

$$C_p = \frac{P_m}{P_1} \quad (3)$$

The power coefficient can be directly expressed as a function of the velocity ratio, as shown in Figure 2.

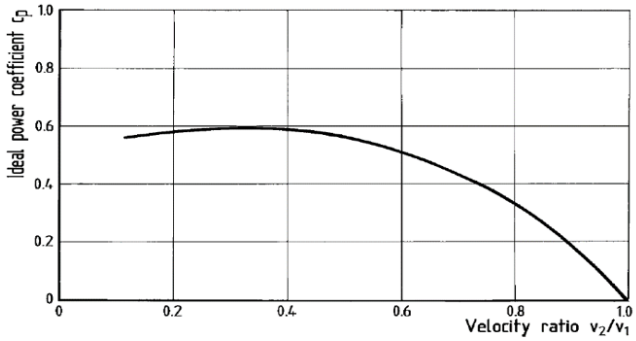

Figure 3: Betz's elementary graph of the relationship between the flow power coefficient and the speed ratio before and after the converter [25]

2.2. Guide channel design

Flow-guiding system used in this study comprised two primary configurations, namely a throat section combined with nozzle (inlet), and another with a diffuser (outlet). These guiding components were designed and fabricated as interchangeable modules to allow comparative analysis of different inlet and outlet angles under consistent throat dimensions.

2.2.1. Nozzle channel configuration

Nozzle configuration had a constant axial length and three inlet angles of 10°, 20°, and 30° to accelerate incoming fluid before passing through the throat and rotor sections, increasing velocity and extractable energy. Figure 4 shows structural details of nozzle and isometric view.

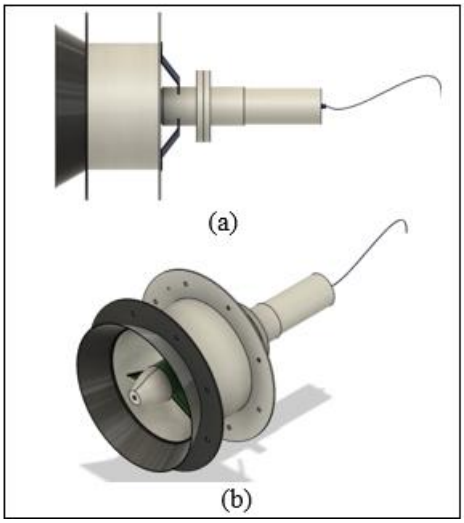

Figure 4: Nozzle model (a) shape of hydrokinetic turbine nozzle channel, (b) isometric shape of the hydrokinetic turbine nozzle channel

Each nozzle ensured a seamless transition from ambient flow to turbine throat, minimizing flow separation and turbulence. The differences in inlet angle were used to investigate how flow convergence affected power extraction and turbine performance.

2.2.2. Diffuser channel configuration

Diffuser expanded flow area after the throat and rotor to create a pressure drop, improving suction and increasing blade-flow velocity. Three diffuser specimens were constructed, each with an outlet angle of 10°, 13.9°, and 15°, respectively, and an identical axial length of 370 mm.

A previous study by [19] using Computational Fluid Dynamics (CFD) identified an outlet angle of 13.9° as optimal, yielding a power coefficient of 98% under ideal conditions (without blade tip clearance) and up to 118% when blade tip clearance was considered. The geometric optimisation of the diffuser outlet in that study used Bezier curve modelling to refine the hydrofoil shape and the flow divergence profile. Another experiment used CFD method based on Response Surface Methodology (RSM) [21] to examine diffuser design and optimization for horizontal-axis hydrokinetic turbine. The results showed that curved portions on diffuser surface could increase flow velocity by approximately 31.7% compared to the case without a diffuser, using a two-dimensional flat airfoil as the basic shape. These findings showed that, in regions with low current speeds, optimizing diffuser design was essential to improve turbine efficiency in terms of energy and flow rate.

In this study, the fabricated diffuser specimens were designed using similar geometric principles to validate CFD-based results under real-flow conditions. Figure 5 shows a visual and isometric rendering of diffuser channel.

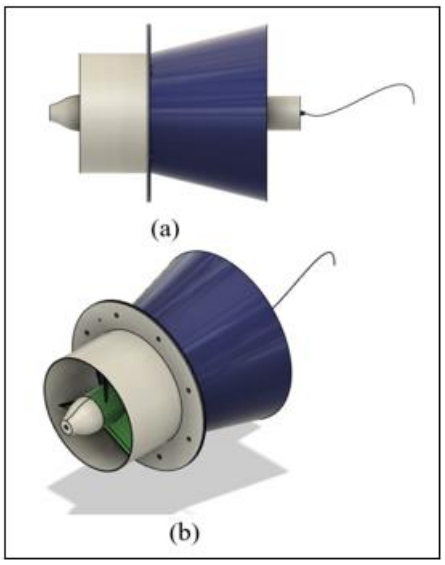

Figure 5: Diffuser model (a) shape of the hydrokinetic turbine diffuser channel, (b) isometric shape of the hydrokinetic turbine diffuser channel

3. Result and Discussion

The performance of nozzle and diffuser channel, each with three angles, connected to a throat of 370 mm, was evaluated at a depth of 1.2 m, with flow velocity adjusted by varying the towing vessel speed. The results showed that nozzle with a 30° inlet angle had the best performance. Meanwhile, diffuser with a 13.9° outlet angle achieved the best performance compared to 10° and 15°.

Figures 6 and 7 show data on the relationship between power mechanics and flow velocity for nozzle and diffuser channel.

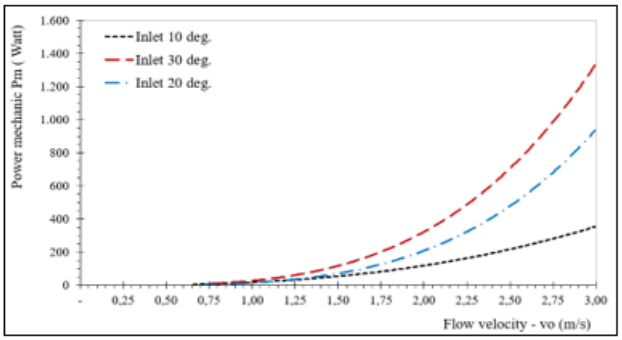

Figure 6: Relationship between power mechanics and flow velocity for each inlet angle.

Based on the results, 30° inlet angle was optimal compared to 20° and 10°. Similarly, a previous study [15] reported that using angles of 30°, 45°, and 60° found an optimal inlet angle of 30°. At an average river flow velocity of 1.6 m/s, the mechanical power extracted by turbine for 30° inlet angle was $P_m(30°) = 150$ W. In comparison, for 20° and 10° inlet angles, the respective values were P_m (20°) = 90 W and P_m (10°) = 75 W.

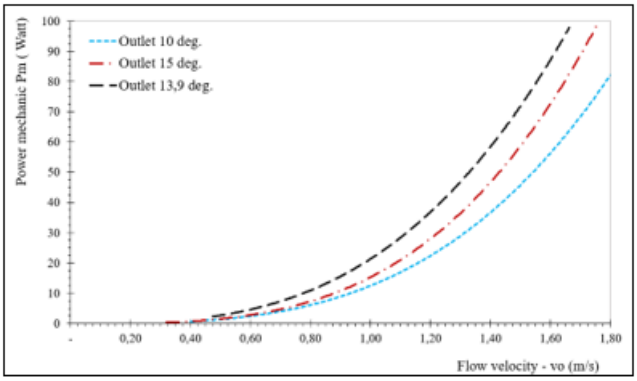

Figure 7: Relationship between power mechanics and flow velocity for each outlet angle.

Figure 7 shows the mechanical power graph for diffuser outlet angles of 10°, 13.9°, and 15°. At the same flow velocity of 1.6 m/s, 13.9° outlet angle produced the highest mechanical power of $P_m(13.9°) = 92$ watts. This value was greater than 10° and 15° angles, which obtained $P_m(10°) = 57$ watts and $P_m(15°) = 73$ watts, respectively. Meanwhile, power coefficients produced by nozzle (C_p) and diffuser (C_p) with varying inlet and outlet angle are shown in Figures 8 and 9.

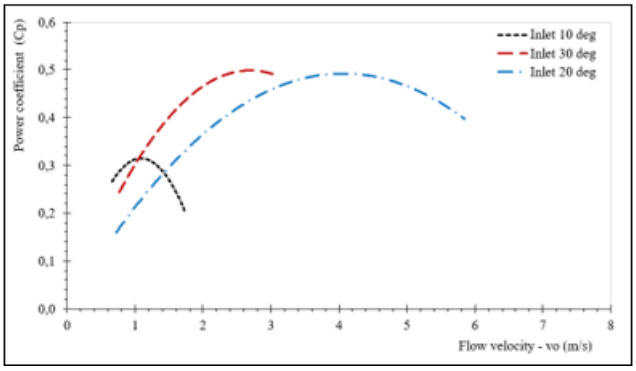

Figure 8: Relationship power coefficient and flow velocity for each inlet angle.

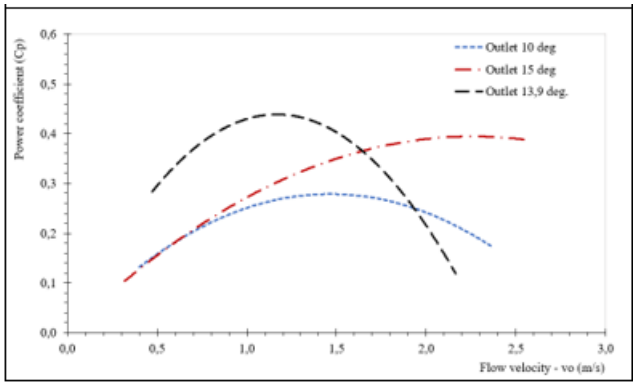

Figure 9: Relationship power coefficient and flow velocity for each outlet angle.

Figure 8 shows the power coefficient alongside with inlet angle from 10°, 20°, and 30°. The highest power coefficient value was obtained at an inlet angle of 30° with $C_p(30°) = 0.51$, followed by $C_p(20°) = 0.48$, and $C_p(10°) = 0.32$ at an average flow velocity of 2.65 m/s, 4.0 m/s, and 1.09 m/s, respectively. Furthermore, using a diffuser channel has increased the power coefficient. As presented in Figure 9, the highest power coefficient occurred at a diffuser outlet angle of 13.9°, with C_p (13.9°) = 0.44, followed by C_p (15°) = 0.39 and C_p (10°) = 0.28, respectively.

The optimal power coefficient for each nozzle and diffuser angle combination and the diffuser channel outlet angles can be determined theoretically from the speed-ratio graphs before and after the blade. Specifically, the addition of nozzle and diffuser channel to the throat channel influences the use of horizontal-axis hydrokinetic turbine, as described in Figure 10.

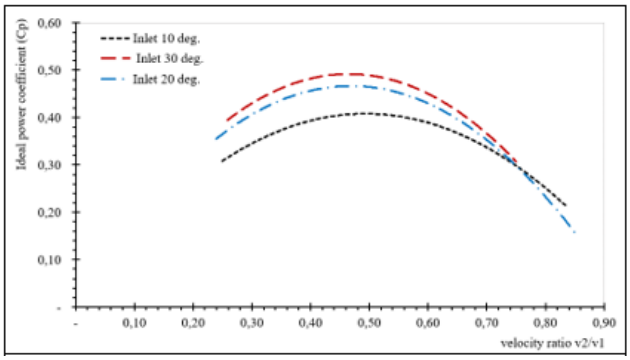

(a)

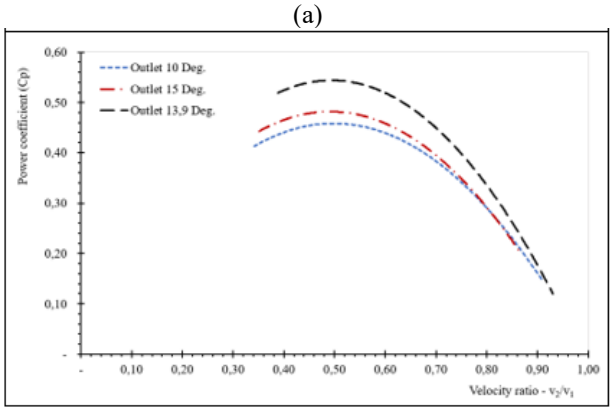

(b)

Figure 10: Relationship between the power coefficient and the ideal to flow velocity ratio (v_2/v_1) (a) for each inlet angle (b) for each outlet angle.

Figures 10(a) and 10(b) show the relationship between the velocity ratio $v_2/v_1$and the corresponding power coefficient. For nozzle configurations, 30° inlet angle showed the highest performance with a power coefficient reaching 0.50. Meanwhile, 13.9° outlet angle achieved a peak theoretical coefficient of approximately 0.54 for diffuser configurations.

The intersection of the mechanical power function line (P_m) with the power coefficient (C_p) shows the optimal point of hydrokinetic turbine using a guide channel. In hydrokinetic turbine using throat guide channel combined with a nozzle and diffuser, the optimal inlet and outlet angles can be plotted on a graph, as shown in Figure 11.

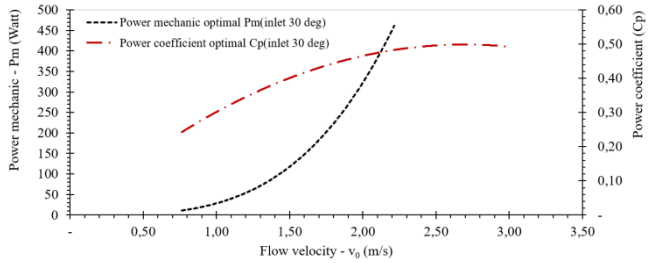

Figure 11: Relationship of power, mechanical, and power coefficient at each change in flow velocity for an inlet angle of 30°

The relationship between turbine performance parameters and flow velocity shows a clear pattern. When turbine operates with optimum inlet nozzle configuration of 30°, both mechanical power and the power coefficient increase with flow velocity, though their growth patterns varied. The power coefficient curve shows a gradual increasing trend in the velocity range of 0.8–2.1 m/s, before finally reaching the optimum condition with a peak value of around 0.50–0.52. The value is close to the theoretical Betz limit, indicating a high level of energy conversion efficiency. This indicates that the guide channel design can accelerate flow, reduce turbulence and improve momentum transfer to the rotor. The result confirms that the contribution of flow velocity to power extraction is much more dominant than the efficiency increases in the medium- and high-operating phases. The point does not indicate the same numerical value, but represents a transition phase in system performance. Meanwhile, the diffuser channel with an outlet angle of 13.9° produces a graph as follows:

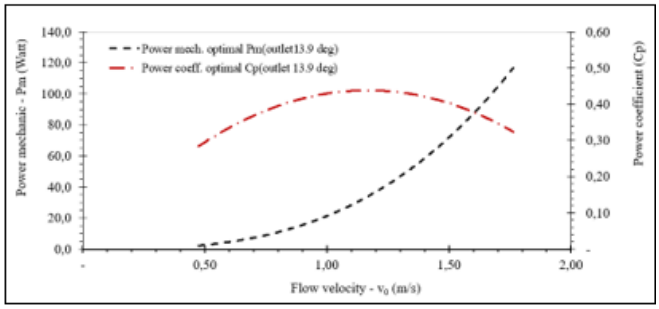

Figure 12: Relationship of power, mechanical and power coefficient at each change in flow velocity for an outlet angle of 13.9°

The performance pattern for the 13. 9° outlet configuration displays a comparable trend, with both mechanical power and power coefficient increasing as flow speed rises, although they respond differently. The power coefficient first climbs within a speed range of roughly 0.6 –1.4 m/s, peaking around 0.43-0.45 before slowly tapering off. This behavior implies that while the diffuser accelerates the flow, the outlet shape at the angle leads to greater flow separation and turbulence at higher speeds, diminishing aerodynamic efficiency.

In comparison, mechanical power increases consistently with flow speed, reaching nearly 120 W at about 1.8–1.9 m/s. Similar to the inlet optimization scenario, this shows that at elevated speeds, power output is primarily determined by the flow's kinetic energy rather than by efficiency improvements.

A significant aspect is the visual point of closeness, where the C_p curve begins to fall while the mechanical power curve continues to climb sharply. Although the method is not a proper mathematical crossing due to the differing axes, it still indicates a change in performance. It shows the operational limit at which any further increase in speed no longer improves conversion efficiency, and where system performance is determined mainly by the available flow energy rather than aerodynamic refinement.

A significant feature of the graph in Figure 12 is the point where the two lines meet, despite being measured on different vertical scales. This intersection does not represent identical numerical values but signals a change in the way the system operates. At this point, the Cp line reaches the saturation level, while the Pm line shows most rapid escalation. Therefore, the point can be considered the threshold at which turbine performance improves, transitioning from primarily driven by increased conversion efficiency to high fluid kinetic energy.

4. Conclusion

In conclusion, this study shows that the performance of ducted hydrokinetic turbine system is significantly affected by differences in inlet nozzle and diffuser outlet angle. The results obtained are as follows:

1) Outperforming the 20° and 10° configurations tested in this study, the 30° inlet nozzle arrangement produces the best performance, with a maximum power coefficient (C_p) of 0.51 at a flow velocity of 2.65 m/s.
2) Among the various diffuser specimens, 13.9° outlet angle has a power coefficient (C_p) of 0.44 at a flow speed of 1.3 m/s.
3) A comparative study shows that although diffuser designs mainly improve flow stabilization and power conversion efficiency, nozzle configurations effectively increase mechanical power output. Specifically, using nozzle geometry, the maximum C_p is approximately 1.25 times that of the best diffuser arrangement.

This study shows that the selection of guide channel form should correlate with the expected design objectives, whether optimizing conversion efficiency or prioritizing mechanical power extraction. The results offer experimental validation for design upgrades for ducted hydrokinetic turbine, particularly for use in slow-moving natural river settings.

References

[1] G. J. IESR, "ASEAN is Still Relying on Fossil Fuel yet Has the Opportunities to Transform its Energy System," JAKARTA, Feb. 2022. Accessed: Jan. 29, 2025. [Online]. Available: https://iesr.or.id/en/asean-is-still-relying-on-fossil-fuel-yet-has-the-opportunities-to-transform-its-energy-system/

[2] C. Klinlampu, N. Chimprang, and J. Sirisrisakulchai, "The sufficient level of growth in renewable energy generation for coal demand reduction," *Energy Reports*, vol. 9, pp. 843–849, Oct. 2023, doi: 10.1016/j.egyr.2023.05.203.

[3] Y. Dou, X. Zhang, and L. Chen, "Research on optimal carbon emissions in the production decision of the coal-fired power plant," *Int. J. Energy Sect. Manag.*, vol. 18, no. 6, pp. 1630–1648, Jan. 2024, doi: 10.1108/IJESM-07-2023-0019.

[4] A. R. Zahedi, S. Labbafi, A. Ghaffarinezhad, and K. Habibi, "Design, Construction and Performance of A Quintuple Renewable Hybrid System of Wind/Geothermal/Biomass/Solar/Hydro Plus Fuel Cell," *Int. J. Hydrogen Energy*, vol. 46, no. 9, pp. 6206–6224, Feb. 2021, doi: 10.1016/j.ijhydene.2020.11.188.

[5] E. Liun, "Potensi Energi Alternatif Dalam Sistem Kelistrikan Indonesia," in *Seminar Nasional Pengembangan Energi Nuklir IV,* INDONESIA: BATAN, 2011, pp. 311–322.

[6] T. E. Rehm, "Advanced nuclear energy: the safest and most renewable clean energy," Mar. 01, 2023, *Elsevier Ltd*. doi: 10.1016/j.coche.2022.100878.

[7] S. Suman, "Hybrid nuclear-renewable energy systems: A review," Apr. 20, 2018, *Elsevier Ltd*. doi: 10.1016/j.jclepro.2018.01.262.

[8] Q. Hassan, S. Algburi, A. Z. Sameen, H. M. Salman, and M. Jaszczur, "A review of hybrid renewable energy systems: Solar and wind-powered solutions: Challenges, opportunities, and policy implications," Dec. 01, 2023, *Elsevier B.V.* doi: 10.1016/j.rineng.2023.101621.

[9] Y. Yao, J.-H. Xu, and D.-Q. Sun, "Untangling Global Levelised Cost of Electricity Based on Multi-Factor Learning Curve for Renewable Energy: Wind, Solar, Geothermal, Hydropower and Bioenergy," *J. Clean. Prod.*, vol. 285, Feb. 2021, doi: 10.1016/j.jclepro.2020.124827.

[10] J. Li *et al.*, "How to Make Better Use of Intermittent and Variable Energy? A Review of Wind and Photovoltaic Power Consumption in China," *Renew. Sustain. Energy Rev.*, vol. 137, 2021, doi: 10.1016/j.rser.2020.110626.

[11] P. Breeze, "The Cost of Electricity From Hydropower Plants," *Hydropower*, pp. 89–93, 2018, doi: 10.1016/b978-0-12-812906-7.00010-7.

[12] S. Adam, A. D. Setiawan, and M. P. Dewi, "Robust geothermal investment decisions under uncertainty: An exploratory financial modeling and analysis approach," *Energy*, vol. 314, Jan. 2025, doi: 10.1016/j.energy.2024.134302.

[13] V. K. Singh and S. K. Singal, "Operation of hydro power plants-a review," Mar. 01, 2017, *Elsevier Ltd*. doi: 10.1016/j.rser.2016.11.169.

[14] B. Kirke, "Hydrokinetic Turbines for Moderate Sized Rivers," *Energy Sustain. Dev.*, vol. 58, pp. 182–195, Oct. 2020, doi: 10.1016/j.esd.2020.08.003.

[15] A. B. Puthumana, "Inlet Shroud Angle of a Shrouded Wind Turbine," *Int. J. Res. Appl. Sci. Eng. Technol.*, vol. V, no. IV, pp. 295–302, Apr. 2017, doi: 10.22214/ijraset.2017.4054.

[16] M. M. Nunes, R. C. F. Mendes, T. F. Oliveira, and A. C. P. Brasil Junior, "An Experimental Study on the Diffuser-Enhanced Propeller Hydrokinetic Turbines," *Renew. Energy*, vol. 133, pp. 840–848, Apr. 2019, doi: 10.1016/j.renene.2018.10.056.

[17] A. Z. Zaidi and M. Khan, "Identifying High Potential Locations for Run-Of-The-River Hydroelectric Power Plants Using GIS and Digital Elevation Models," Jun. 01, 2018, *Elsevier Ltd*. doi: 10.1016/j.rser.2018.02.025.

[18] D. A. T. D. do Rio Vaz, J. R. P. Vaz, and P. A. S. F. Silva, "An approach for the optimization of diffuser-augmented hydrokinetic blades free of cavitation," *Energy Sustain. Dev.*, vol. 45, pp. 142–149, Aug. 2018, doi: 10.1016/j.esd.2018.06.002.

[19] T. J. Rezek, R. G. R. Camacho, N. M. Filho, and E. J. Limacher, "Design of a Hydrokinetic Turbine Diffuser Based on Optimization and Computational Fluid Dynamics," *Appl. Ocean Res.*, vol. 107, Feb. 2021, doi: 10.1016/j.apor.2020.102484.

[20] M. M. Nunes, A. C. P. Brasil Junior, and T. F. Oliveira, "Systematic review of diffuser-augmented horizontal-axis turbines," *Renew. Sustain. Energy Rev.*, vol. 133, pp. 1–22, Nov. 2020, doi: 10.1016/j.rser.2020.110075.

[21] W. Khalid, S. Sherbaz, A. Maqsood, and Z. Hussain, "Design and optimization of a diffuser for a horizontal axis hydrokinetic turbine using computational fluid dynamics based surrogate modelling," *Mechanika*, vol. 26, no. 2, pp. 161–170, Apr. 2020, doi: 10.5755/j01.mech.26.2.23511.

[22] K. Song, W. Q. Wang, and Y. Yan, "Numerical and experimental analysis of a diffuser-augmented micro-hydro turbine," *Ocean Eng.*, vol. 171, pp. 590–602, Jan. 2019, doi: 10.1016/j.oceaneng.2018.12.028.

[23] A. Aranake and K. Duraisamy, "Aerodynamic Optimization of Shrouded Wind Turbines," *Wind Energy*, vol. 20, no. 5, pp. 877–889, May 2017, doi: 10.1002/we.2068.

[24] A. Agha, H. N. Chaudhry, and F. Wang, "Determining the Augmentation Ratio and Response Behaviour of a Diffuser Augmented Wind Turbine (DAWT)," *Sustain. Energy Technol. Assessments*, vol. 37, Feb. 2020, doi: 10.1016/j.seta.2019.100610.

[25] Hau Erich, *Wind Turbines (Fundamentals, Technologies, Application, Economics)*, 2nd ed. Munich, Germany: Springer, 2005.